

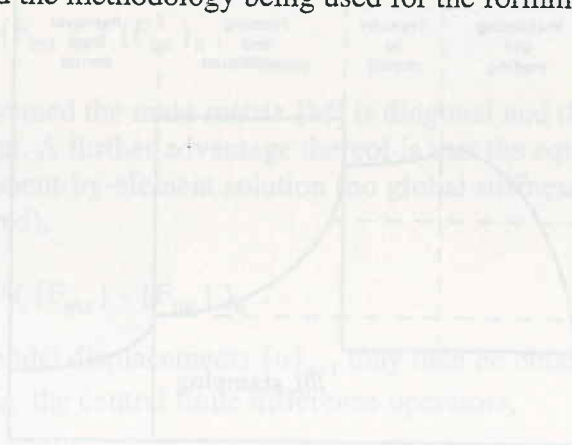
**Title: Industrial Press Forming of Continuous Fibre Reinforced Thermoplastic Sheets and the Development of Numerical Simulation Tools**

**Authors: A.K Pickett, T. Queckbörner, P. De Luca and E. Haug**  
**Engineering System International,**  
**Frankfurter Str 13-15,**  
**D-65760 Eschborn, Germany.**

The pressure forming, or "Thermoforming", of pre-consolidated continuous fibre reinforced thermoplastic (FRTP) sheets offers a promising fabrication option for structural composite components in both the transportation and manufacturing industries. Modern thermoplastic polymers have improved mechanical and physical properties compared to their thermoset counterparts giving greater toughness, impact tolerance and, perhaps most important for industry, the possibility for rapid part production using the stamping method.

As in traditional metal stamping the current process and part design for thermoforming rely heavily on "trial and error" practices which are costly, inefficient and provide little scope for optimization and understanding of the forming process. This paper describes the aims and preliminary results of a Brite-Euram project which will develop numerical software tools for the CAE (computer aided engineering) design of the part and thermoforming stamping process.

The software tools are based on a pre-heating analyser to determine the three dimensional temperature distribution in the anisotropic sheet and a forming analyser to simulate the forming and the cooling process. Final part shape will include such information as part thickness distributions, fibre orientations, material defects and a prediction of residual deformations due to cooling (thermal) effects. This paper will present some preliminary results and the methodology being used for the forming operation.



## 1. Introduction

Structural thermoplastics having continuous fibre reinforcement embedded in a thermoplastic matrix (FRTP) offer advantages that make this class of material of interest to both transport and manufacturing industries. For industrial applications perhaps the most important advantage is the possibility of rapid part forming using the 'stamping' approach [1]. This allows cycle times which are much faster than thermoset based composites and begin to compete with traditional metal stamping.

During metal stamping the blank undergoes large plastic straining; unsatisfactory forming may include material tearing, wrinkling, or excessive springback. In contrast the stamping of thermoplastic components from sheets of pre-consolidated long fibre reinforced material requires very different deformation modes within the material to form the final shape [2]. The stacked plies may either slide over each other (interply sliding), or each ply may deform independently. Due to the constraining effect of the stiff continuous fibre reinforcement ply deformation is essentially restricted to the intraply shearing mode.

With reference to Figure 1, three stages of the thermoforming process may be identified. Firstly a 'pre-heating' of the pre-form sheet is necessary to obtain a uniform and sufficiently high temperature distribution above the matrix melt temperature  $T_m$ . The location, means and duration of the heating sources are process variables to be considered. During the second stage a stamping operation is made. Usually the forming tools are maintained at temperatures below a solidification temperature  $T_s$  in order to speed cooling and reduce cycle times. A fast stamping operation is therefore essential to avoid material solidification during forming. The final stage involves cooling the part in the tools to a temperature where sufficient internal material strength is generated so that the part remains dimensionally stable during extraction from the mould and further cooling.

Sources of processing and part failure include, among others, excessive heat exposure during pre-heating leading to material degradation or, alternatively, insufficient heating which will cause subsequent forming problems. During stamping material failure may include fibre breakage or buckling. The final part quality is largely dependent on the cooling conditions. The applied pressure and cooling rate control the development of morphological defects and the buildup of internal stresses.

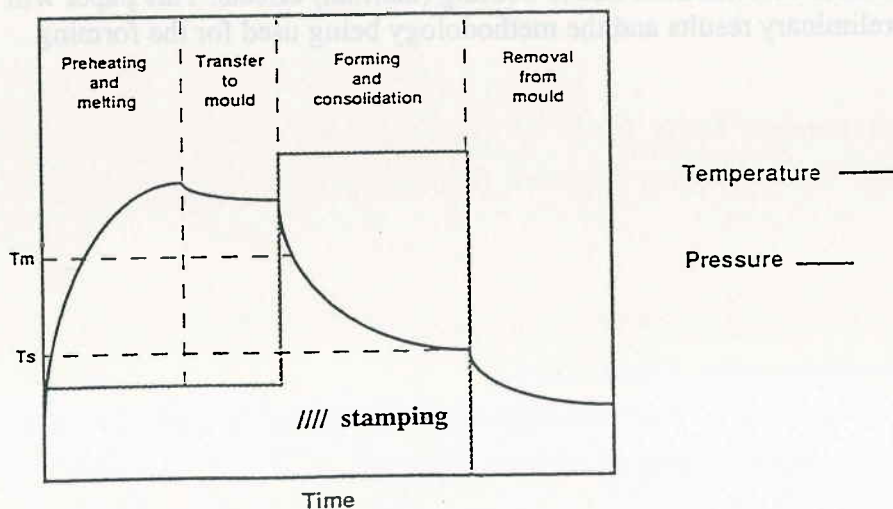


Fig 1: Principle stages of pressure and temperature in the processing of pre-consolidated FRTP sheets, Ref [2].



During each of the above forming stages the correct processing and material variables are needed to ensure a good final part quality. Clearly the desire to reduce cycle times will lead to compromises in both the processing conditions and final part quality. Numerical analysis methods may be used to help guide the choice of processing conditions and avoid difficult and costly 'trial and error' testing methods. For this reason a present Brite-Euram project [3] is developing necessary software tools to investigate each stage of the thermoforming process. This paper will present some preliminary results and the methodology being developed for the stamping stage only. Here an explicit finite element method with heat conduction capabilities is being developed.

## 2. The Explicit Finite Element Method

In general two formulations for a finite element analysis are possible, namely the implicit and explicit methods. The Implicit is more common and used in a wide range of general purpose codes for the solution of linear and non linear problems. In recent years the explicit method has proven successful for the analysis of specific highly nonlinear dynamic problems, particularly where contact of different parts is involved [4]. Automotive crashworthiness and metal stamping are two notable applications.

Briefly the explicit Finite Element method may be described as follows. Essentially standard finite elements are used to discretize a structure and formulate the linearized equations of motion at a particular instance of time,

$$[M]\{\ddot{u}\}_n + [C]\{\dot{u}\}_n + [K]\{u\}_n = \{F_{ext}\}_n$$

where;

$\{u\}$ ,  $\{\dot{u}\}$  and  $\{\ddot{u}\}$  are the nodal displacement, velocity and acceleration vectors,  
 $n$  is the cycle, or iteration, at a time position  $T_n$  after  $n\Delta T$  timesteps,  
 $[M]$ ,  $[C]$  and  $[K]$  are the mass, damping and stiffness matrices respectively, and  
 $\{F_{ext}\}$  is a vector of external applied nodal forces.

It is usual to ignore the effects of material damping and, replacing the term  $[K]\{u\}_n$  with the equivalent internal nodal forces vector  $\{F_{int}\}$ , gives Newton's second law of motion,

$$[M]\{\ddot{u}\}_n = \{F_{ext}\}_n - \{F_{int}\}_n.$$

If a lumped mass distribution is assumed the mass matrix  $[M]$  is diagonal and the solution for nodal accelerations  $\{\ddot{u}\}$  is trivial. A further advantage thereof is that the equations become uncoupled allowing an element-by-element solution (no global stiffness matrix assembly, or its inversion, is required),

$$\{\ddot{u}\}_n = [M]^{-1} (\{F_{ext}\}_n - \{F_{int}\}_n). \quad (1)$$

The nodal velocities  $\{\dot{u}\}_{n+1/2}$  and nodal displacements  $\{u\}_{n+1}$  may then be obtained by integration in the time domain using the central finite difference operators,

$$\begin{aligned} \{\dot{u}\}_{n+1/2} &= \{\dot{u}\}_{n-1/2} + \{\ddot{u}\}_n \Delta T_n \\ \{u\}_{n+1} &= \{u\}_n + \{\dot{u}\}_{n+1/2} \Delta T_{n+1/2}. \end{aligned} \quad (2)$$

Equations (1) and (2) are 'conditionally stable' requiring a maximum allowable timestep

$\Delta T_{\text{critical}}$  which is dependent on element size and material properties. The above system of equations provides a solution algorithm which is most effective for highly non-linear dynamic problems having a relatively short time duration. Further discussions on the implicit and explicit algorithms, and their relative merits are given in [5]. In the case of thermoforming, interface contact between plies and the tools can only be effectively treated using an explicit analysis.

### 3. Metal Stamping Simulation - State of the Art

The potential to save development time and costs through computer simulation of the metal stamping process has been a driving factor in its evolution over the past five years. Presently complex steel or aluminium parts may be analysed having either a one or multi-step stamping operation. As yet the most promising simulation tools are based on the explicit finite element method and one industrial code under development is PAM-STAMP [6]. Figure 2 shows a typical simulation setup and final stamping results. Information obtainable includes final (residual) stress and strain distributions, possible material tearing and the prediction of elastic springback. These simulation techniques are currently at a level of first industrial application. The main drawback at present is the generation of the finite element mesh which is still very labour intensive. In future effective links between the CAD data and finite element mesh generation will be developed.

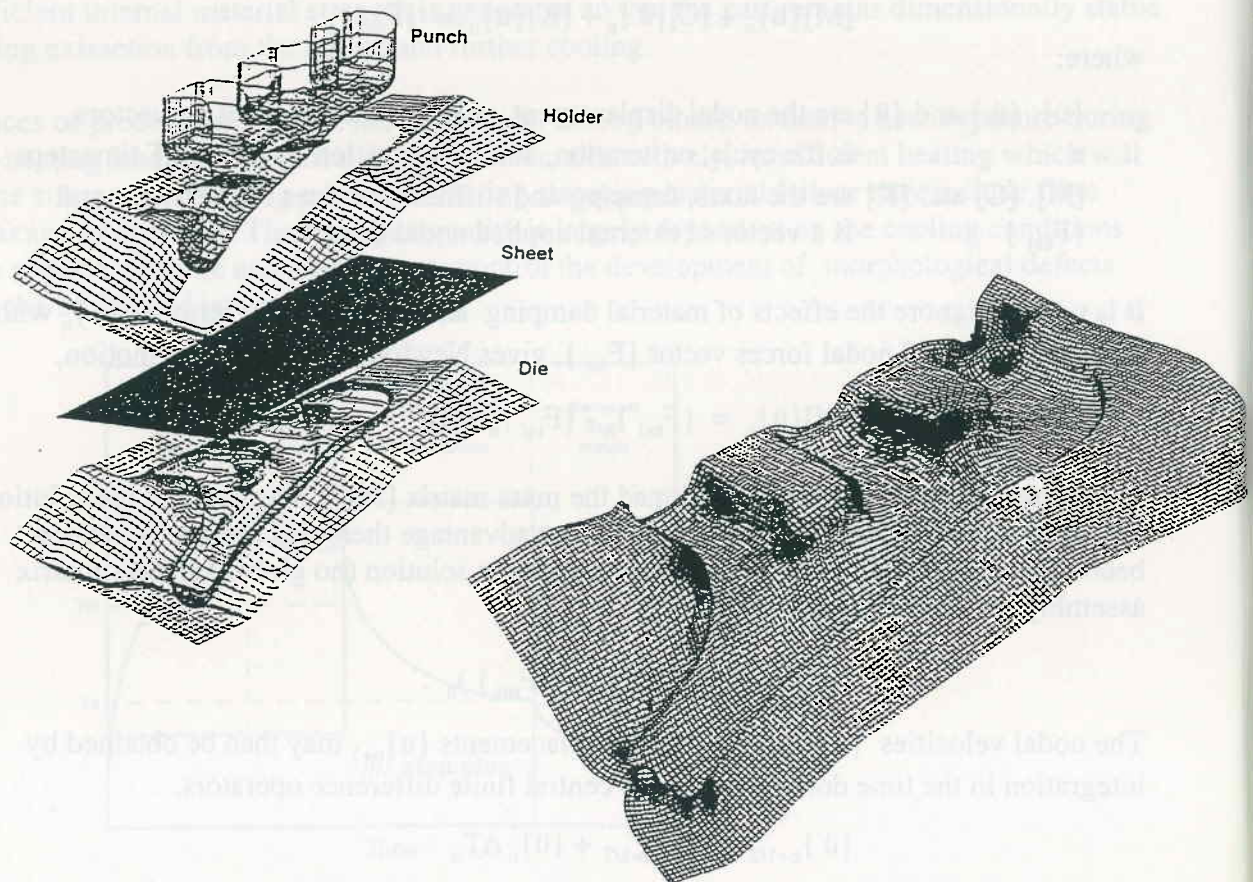


Fig 2: Typical setup for a metal stamping simulation and example results of elasto-plastic strain distribution (courtesy of Leistrizt)



#### 4. The Bi-Phase Thin Shell Element

Considering the deformations that the laminate must undergo during thermoforming it is necessary to enable both intraply shearing of each ply and interply shearing between the plies. A single shell finite element cannot model the interply shearing effects and, consequently, the approach adopted here is to stack thin shell elements in order to idealize the laminate. Each thin shell represents one ply and the relative sliding between plies is controlled by an interface treatment in which sliding constraints are imposed and penalized using a viscous dependent friction law.

In each element a 'bi-phase' material law is used where a linear elastic phase represents the unidirectional fibres and a viscous phase represents the matrix. The formulation is similar to [7] excepting that the implementation is in a three dimensional thin shell element and the simplification of inextensible fibres is replaced using a linear elastic model. At present only unidirectional fibres (APC2 type materials) are considered. Briefly the element constitutive law defined in the element fibre frame is as follows:

$$\sigma_{ij} = \sigma_{ij \text{ viscous}} + \sigma_{ij \text{ elastic}}$$

$$\begin{bmatrix} \sigma_{11} \\ \sigma_{22} \\ \sigma_{12} \end{bmatrix} = \underbrace{\begin{bmatrix} 4\eta_L & 2\eta_T & 0 \\ 2\eta_T & 4\eta_T & 0 \\ 0 & 0 & 2\eta_L \end{bmatrix}}_{\text{viscous part}} \begin{bmatrix} \dot{\epsilon}_{11} \\ \dot{\epsilon}_{22} \\ \dot{\epsilon}_{12} \end{bmatrix} + \underbrace{\begin{bmatrix} E_{\text{Ply}} & 0 & 0 \\ 0 & 0 & 0 \\ 0 & 0 & 0 \end{bmatrix}}_{\text{elastic part}} \begin{bmatrix} \epsilon_{11} \\ \epsilon_{22} \\ \epsilon_{12} \end{bmatrix}$$

where  $\sigma_{ij}$  = element stress components,  
 $\epsilon_{ij}$  = are the corresponding element strain components,  
 $\dot{\epsilon}_{ij}$  = are the element strain rate components,  
 $\eta_L$  and  $\eta_T$  = longitudinal (fibre direction) and transverse matrix viscosity coeff,  
 $E_{\text{ply}}$  = fibre elasticity modulus.

#### 5. Simple Examples of Inplane Thermoforming

The simulation of two simple inplane thermoforming problems is demonstrated. In each case solutions are compared with published numerical results from [7,8] where an implicit two dimensional (plane stress) finite element code was used. These results were in turn validated using classical analytical and experimental testing.

##### 5.1 A Simple Cantilever Beam

A cantilever beam made from a single ply of APC2 material and subjected to axial inplane loading is investigated. The following typical material properties are used:

$$\begin{aligned} E_{\text{fibres}} &= 130 \text{ GN/m}^2 && (\text{Ref [7] assumes inextensibility}) \\ \eta_L &= 6000 \text{ N s m}^{-2} \\ \eta_T &= 3500 \text{ N s m}^{-2} \end{aligned}$$

The geometry, constraints, loading and fibre orientations of the problem are shown in Figure 3a. The fibre orientation is at  $45^\circ$  to the beam axis. Comparison results for thickness distribution in the deformed ply are shown in figure 3b, where it may be seen that the constraints imposed by the off-axis fibre orientation causes shear deformations and nonuniform loading within the ply. Generally the results show a close agreement however some differences do result probably due to the different elements and algorithms being used. Also, for numerical reasons, Reference [7] assumes fibre inextensibility whereas the explicit approach allows the correct fibre stiffness to be defined.

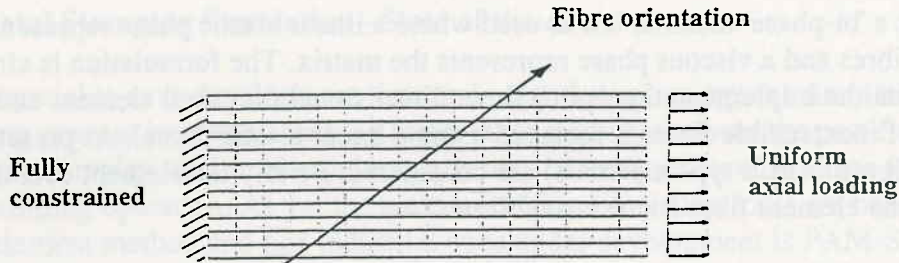
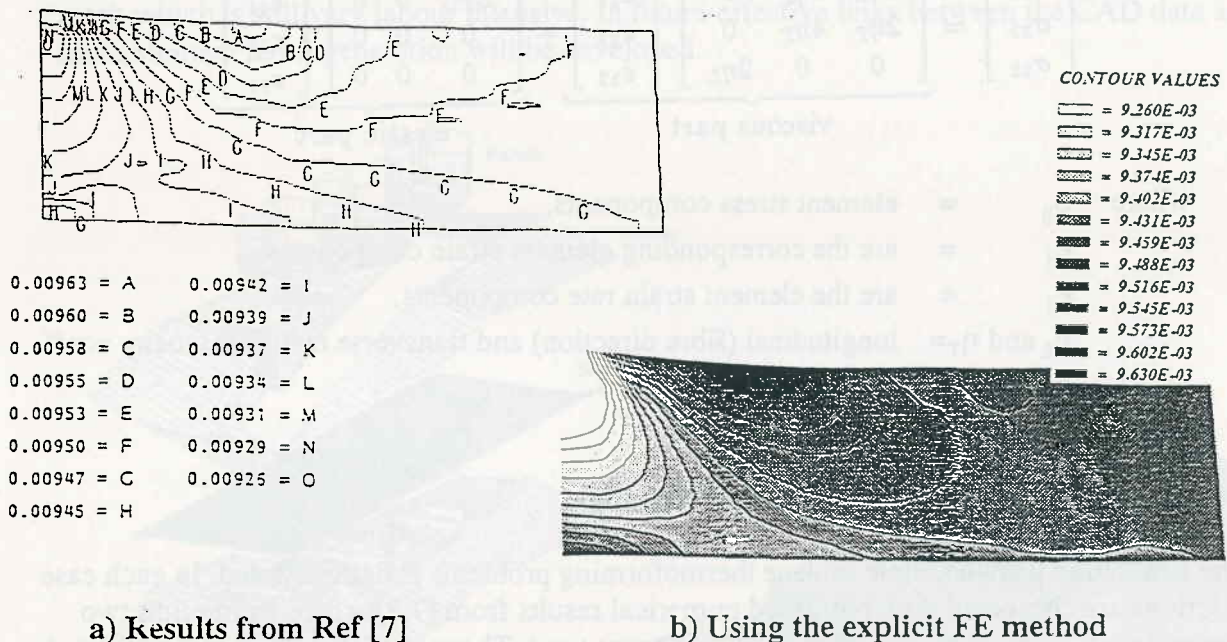


Fig 3a: Constraints, loading geometry and fibre orientation for the cantilever beam test case



a) Results from Ref [7]

b) Using the explicit FE method

Fig 3b: Comparison results of thickness distributions for the cantilever beam test case with  $45^\circ$  fibres under uniform axial loading

## 5.2 Central Indentation of a Circular Sheet

A single ply of APC2 material in the form of a disc of 8.5 inches diameter is loaded by a punch of 1 inch diameter. The punch loading is approximated by imposing an inward radial velocity. Only one symmetric quarter of the problem as shown in Figure 4a was analysed. In this study the fibres run in the y direction and the following material data was used:



$$\begin{aligned}
 E_{\text{fibres}} &= 130 \text{ GN/m}^2 && (\text{Ref [8] assumes inextensibility}) \\
 \eta_L &= 6000 \text{ N s m}^{-2} \\
 \eta_T &= 4000 \text{ N s m}^{-2} .
 \end{aligned}$$

Comparison result for inplane shear and normal stress (in the fibre direction) are given in figures 4b and 4c respectively. Generally a good agreement is obtained although some differences do exist probably for the reasons noted above. A full discussion of these results, and the loading mechanisms, is given in Reference [8].

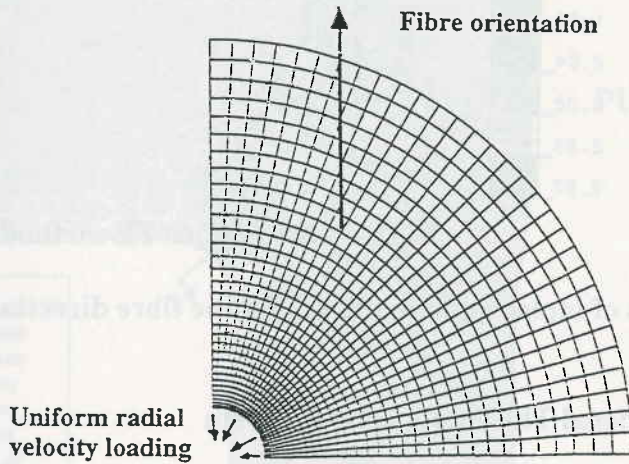
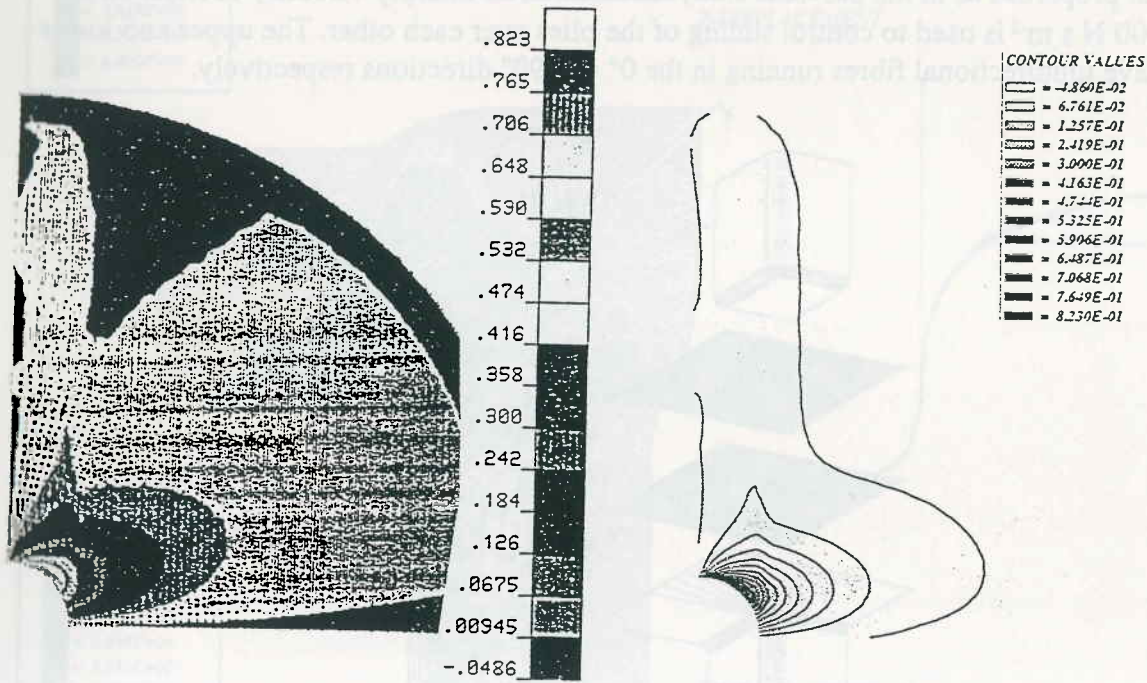


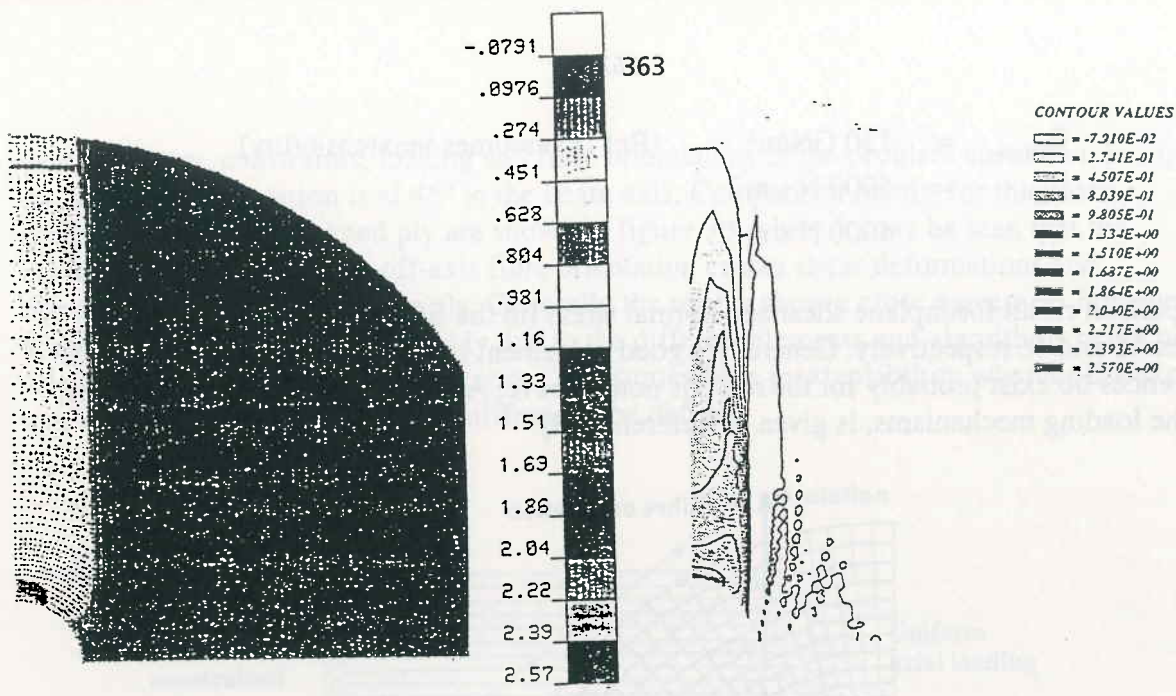
Fig 4a: Constraints, loading, geometry and fibre orientation



a) Results from Ref [8]

b) Using the explicit FE method

Fig 4b: Comparison results of inplane shear stress



a) Results from Ref [8]

b) Using the explicit FE method

Fig 4c: Comparison results of inplane normal stress (in the fibre direction)

### 6. Example of a Three Dimensional Thermoforming Problem

An example of a full three dimensional forming problem using a 'butterdose' study is presented in Figure 5a. For this simplified study only two plies are considered have the same material properties as in the previous study. In addition an interply viscosity coefficient of  $\eta = 4000 \text{ N s m}^{-2}$  is used to control sliding of the plies over each other. The upper and lower plies have unidirectional fibres running in the  $0^\circ$  and  $90^\circ$  directions respectively.

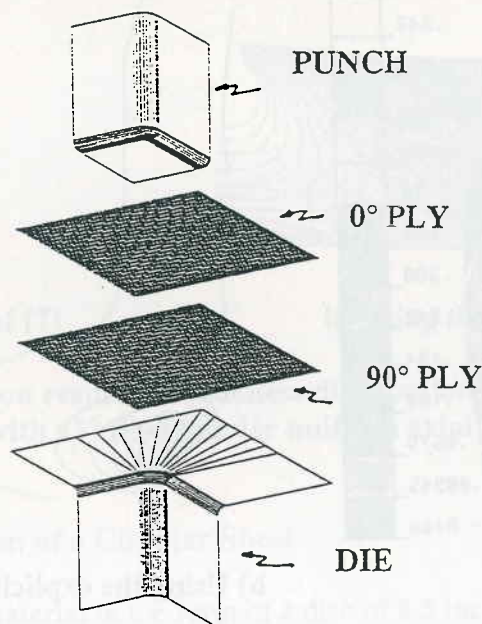


Fig 5a: Setup for the three dimensional thermoforming problem



Figure 5b shows two deformation states of the forming of the laminate into the rectangular box. It may be seen that the constraining effects of the stiff reinforcing fibres restricts the ability of the plies to deform, particularly in the corner. During the later stages of forming local buckling of the plies starts to occur together with a separation of the plies from the die upper face. Significant intraply shearing of both plies has also occurred on the upper surface close to the corner.

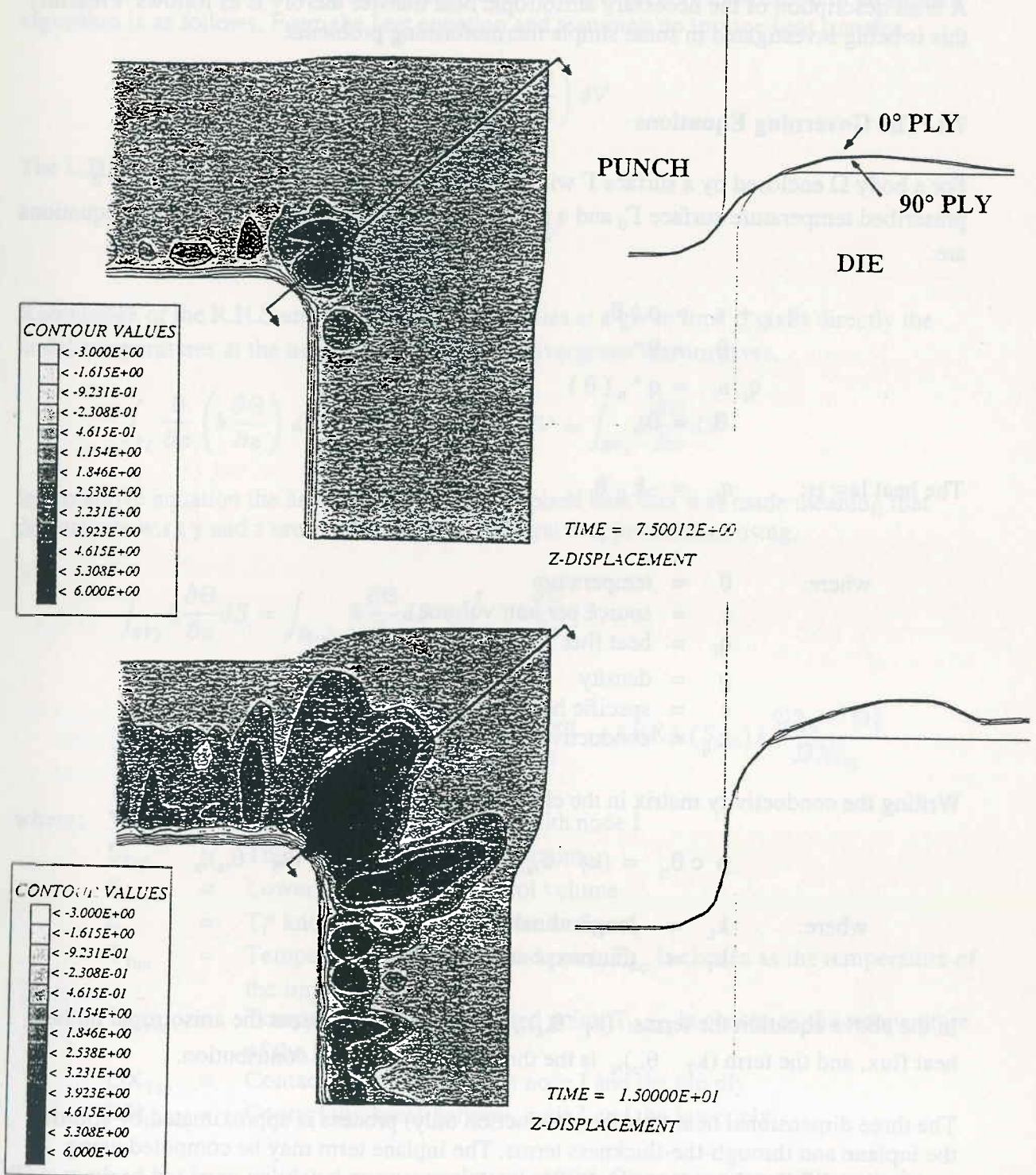


Fig 5b: Example results (contours of vertical deformation and section deformation plots) at two states for the three dimensional thermoforming problem

## 7. The Heat Conduction Equations

An important aspect of the thermoforming stamping simulation is the coupled heat conduction analysis and the critical role temperature effects have on the material and process parameters. Heat conduction transfer during stamping is rapid due to contact of the hot sheet with the cool tooling and highly anisotropic due to the nature of the fibre reinforced material. A brief description of the necessary anisotropic heat transfer theory is as follows. Presently this is being investigated in some simple thermoforming problems.

### 7.1 The Governing Equations

For a body  $\Omega$  enclosed by a surface  $\Gamma$  with a unit normal  $n$  which is subdivided into a prescribed temperature surface  $\Gamma_\theta$  and a prescribed flux surface  $\Gamma_q$ . The governing equations are:

$$\begin{aligned} -q_{i,i} + s &= \rho c \theta_{,t} && \text{in } \Omega \\ \theta &= \theta^* && \text{on } \Gamma_\theta \\ q_i n_i &= q^* n_i(\theta) && \text{on } \Gamma_q \\ \theta &= \theta_o && \text{in } \Omega \text{ when } t = 0 \end{aligned}$$

The heat law is:  $q_i = -k_{ij} \theta_{,j}$

where:

- $\theta$  = temperature
- $s$  = source per unit volume
- $q_i$  = heat flux
- $\rho$  = density
- $c$  = specific heat
- $k_{ij}$  = conductivity matrix

Writing the conductivity matrix in the element fibre direction  $y$  gives,

$$\rho c \theta_{,t} = (k_T \theta_{,x})_{,x} + (k_L \theta_{,y})_{,y} + (k_T \theta_{,z})_{,z}$$

where:

- $k_L$  = longitudinal conductivity
- $k_T$  = transverse conductivity.

In the above equation the terms  $(k_T \theta_{,x})_{,x} + (k_L \theta_{,y})_{,y}$  represent the anisotropic inplane heat flux, and the term  $(k_T \theta_{,z})_{,z}$  is the through-the-thickness contribution.

The three dimensional heat transfer (conduction only) process is approximated by splitting the inplane and through-the-thickness terms. The inplane term may be computed using conventional finite element methods [9].



The through-the-thickness contribution accounts for heat transfer between neighbouring plies and between the ply to tool contact. Here the problem is to transfer heat between element which are not interconnected but are in mechanical contact. For this a 'finite volume' like technique is used [10]. Essentially this method integrates the partially differential equations that govern the phenomena over a control volume associated with each node of the mesh. A 2D example of the control volume is depicted in Figure 6a, for a shell element the thickness must be taken into account, Figure 6b. The theory suitable for implementation in an explicit algorithm is as follows. From the heat equation and assuming no inplane heat transfer,

$$\int_{V_I} \rho C \frac{\partial \Theta}{\partial t} dV = \int_{V_I} \frac{\partial}{\partial x} \left( k \frac{\partial \Theta}{\partial x} \right) dV$$

The L.H.S is approximated by:

$$\frac{1}{\Delta t_{n-1/2}} [\Theta_I^{n+1} - \Theta_I^n] \int_{V_I} \rho C dV$$

Knowledge of the R.H.S and of the various quantities at a given time  $t_n$  gives directly the nodal temperatures at the next timestep  $t_{n+1}$ . The divergence theorem gives,

$$\int_{V_I} \frac{\partial}{\partial x} \left( k \frac{\partial \Theta}{\partial x} \right) dV = \int_{V_I} \text{div} \left( k \frac{\partial \Theta}{\partial x} \right) dV = \int_{\partial V_I} k \frac{\partial \Theta}{\partial x} dS$$

In the above equation the assumption of a null in-plane heat flux was made meaning that derivatives w.r.t y and z are zero. Finally the integral is approximated using,

$$\int_{\partial V_I} k \frac{\partial \Theta}{\partial x} dS = \int_{S_{\text{lower}}} k \frac{\partial \Theta}{\partial x} dS + \int_{S_{\text{top}}} k \frac{\partial \Theta}{\partial x} dS$$

$$\int_{\partial V_I} k \frac{\partial \Theta}{\partial x} dS \simeq \text{AREA}(S_{\text{lower}}) k \frac{\Theta_I^n - \Theta_{\text{lower}}^n}{DX_{\text{lower}}} - \text{AREA}(S_{\text{top}}) k \frac{\Theta_{\text{top}}^n - \Theta_I^n}{DX_{\text{top}}}$$

- where:
- $V_I$  = Control volume associated with node I
  - $S_{\text{Top}}$  = Top surface of the control volume
  - $S_{\text{Lower}}$  = Lower surface of the control volume
  - $t_I$  =  $T_I^n$  known nodal temperature at time  $t_n$
  - $T_{\text{Top}}$  = Temperature of the impacted point,  $T_{\text{top}}$  is chosen as the temperature of the impacted element
  - $T_{\text{Lower}}$  = Temperature of the impacted point,  $T_{\text{Lower}}$  is chosen as the temperature of the impacted element
  - $DX_{\text{Top}}$  = Contact thickness between node I and the top ply
  - $DX_{\text{Lower}}$  = Contact thickness between node I and the lower ply

This method has been validated against analytical results. Since it is compatible with the inplane treatment [9] a full heat conduction analysis of the thermoforming problem within the explicit finite element method is possible.

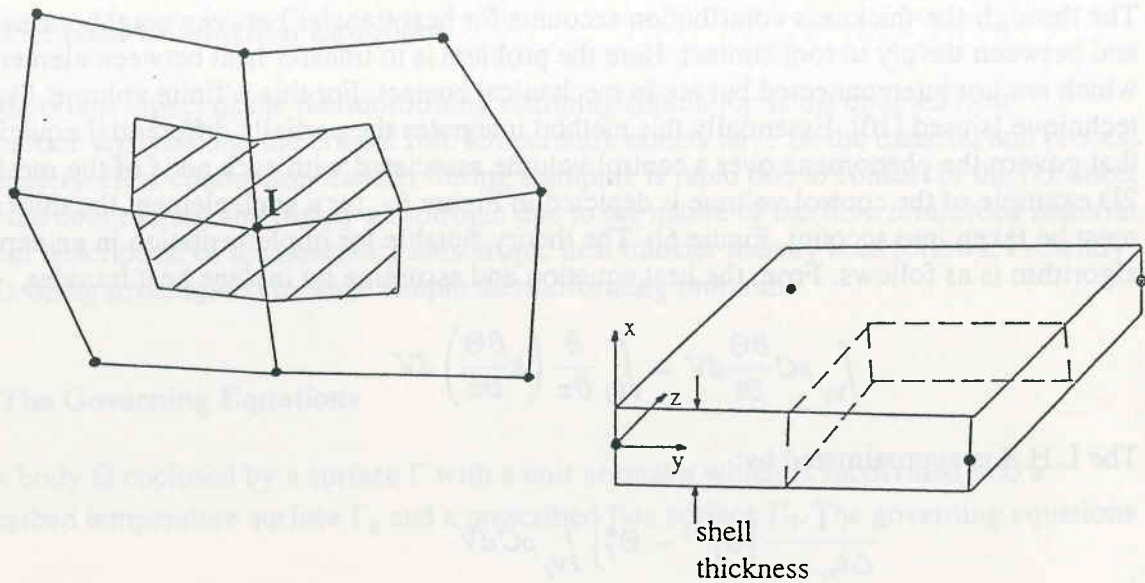


**Fig 6:** a) 2D example of the control volume associated with node I  
 b) Part of the control volume for a shell element

## 8. Conclusions

A simulation method suitable for the thermoforming of laminated composites has been presented based on the explicit finite element method. The laminate has been modelled using stacked thin shell elements with interface constraints. Using this approach all important deformation modes of the laminate during forming, including interply and intraply shearing, may be represented.

First results for the case of isothermal forming have been presented which compare well with other published results. The principles have also been demonstrated for the case of a full three dimensional forming problem, although full validation work still remains to be done.

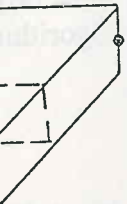
Finally the theoretical basis for the implementation of the heat conduction in the explicit method has been outlined.

## Acknowledgements

The authors would like to thank all of the partners involved in Brite-Euram project BE-5092 and the European Commission for their support.



## References

- 
- [1] Manson, J.-A.E., "Processing of Thermoplastic-Based Advanced Composites", in 'Advanced Thermoplastic Composites: Characterization Processing', Ed. H.H. Kausch, Hanser Publ., pp. 273-301, 1993.
- [2] Cogswell, F.N., "Thermoplastic Aromatic Polymer Composites", Butterworth Heinemann Publ., 1992.
- [3] Brite-Euram Project No. BE-5092, "Industrial Press Forming of Continuous Fibre Reinforced Thermoplastic Sheets and the Development of Numerical Simulation Tools".
- [4] Pickett, A.K., et al, "Some Recent Developments in Numerical Crashworthiness Simulation", Conference: XXII International Finite Element Congress, Baden-Baden Germany, 15/16 Nov. 1993.
- [5] Cook, R. D., Malkus, D. S. and Plesha, M.E., "Concepts and Applications of Finite Element Analysis", Wiley Publ., 1989.
- [6] The PAM-STAMP code, Engineering Systems International SA, 20 Rue Saarinen, Silic 270, 94578 Rungis-Cedex, France.
- [7] O' Brádaigh, C.M. and Pipes, R.B., "Finite Element Analysis of Composite Sheet Forming Process", Composites Manufacturing, Vol 2, No 3/4, pp 161-170, 1991.
- [8] O' Brádaigh, C.M., McGuinness, G.B. and Pipes, R.B., "Numerical Analysis of Stresses and Deformations in Composite Materials Sheet Forming: Central Indentation of a Circular Sheet", Composites Manufacturing, 1993.
- [9] Belytschko, T. and Liu, W.K., "Efficient Linear and Nonlinear Heat Conduction with a Quadrilateral Element", International Journal for Numerical Methods in Engineering, Vol 20, pp 931-948, 1984.
- [10] Peyret, P., "Numerical Methods in Fluid Dynamics", Springer-Verlag Publ., 1983.